MASTER OF PHILOSOPHY, Modelling of Materials

Friday 26th April 2002 9 – 12

MODELLING OF MATERIALS (2) – possible Answers

SECTION A

1. (a) $\mathbf{a}_2 \wedge \mathbf{a}_3$ defines a vector pointing normal to the (1 0 0) plane whose magnitude is $a_2 a_3 \sin\alpha$ where α is the angle between $\mathbf{a}_2$ and $\mathbf{a}_3$. This magnitude is therefore the area of the (1 0 0) plane. Dotting $\mathbf{a}_2 \wedge \mathbf{a}_3$ with $\mathbf{a}_1$ has the effect of multiplying the area of the (1 0 0) plane with the height of the unit cell, thereby giving the volume of the unit cell (Fig. 1).

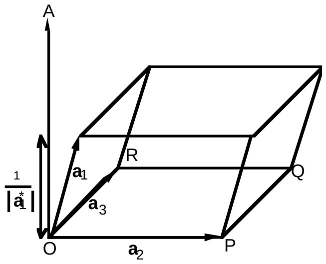

Fig. 1: a_1^* lies along the direction $\underline{\text{OA}}$ and the volume of the parallelepiped formed by the basis vectors a_i is given by $a_1.a_2\wedge a_3$, the area OPQR being equal to $|a_2\wedge a_3|$.

(b) The Poisson's ratio is defined as:

$$\nu = -\frac{\epsilon_{\text{lateral}}}{\epsilon_{\text{longitudinal}}}$$

where ϵ represents elastic strain along the appropriate direction.

Consider a sample of dimensions x, y, z. Deform by Δx, Δy, and Δz respectively. Given uniaxial tension, it follows that

$$\Delta x = \epsilon x \qquad \Delta y = -\nu\epsilon y \qquad \Delta z = -\nu\epsilon z$$

where ϵ is the elastic strain along x. Conservation of volume requires that:

$$\begin{aligned} xyz &= (x+\epsilon x)(y-\nu\epsilon y)(z-\nu\epsilon z) \\ 1 &= (1+\epsilon)(1-\nu\epsilon)(1-\nu\epsilon) \\ 0 &= \epsilon - 2\nu\epsilon \\ 0 &= 1-2\nu \qquad \text{if} \qquad \nu = \frac{1}{2} \end{aligned}$$

(c) The post–iterative heat accumulation technique can be used to account for latent heat evolution (or absorption) during numerical simulation of heat transfer. This technique is based on artificially holding the temperature of the element undergoing the phase change at the transformation temperature until the amount of (specific) heat discounted by doing this has reached that corresponding to the latent heat of the transformation. Further heat flow is then permitted to generate temperature changes

(d) Molecular solids – spherical charge distribution similar to free atoms. Weak attractive van der Waals interaction. Spherically symmetric radial potential.

Ionic solids - near spherical distribution but charge transfer occurs to fill electron shells. This results in anions and cations. Therefore principal potential is Coulombic ($\simeq 1/r$). Spherically symmetric and radial.

Covalent solids – distribution is localised in certain preferred directions forming “chemical bonds”. Bonding electrons are provided by a “promotion” process within the electron shells.

Metallic solids - covalent bond expands so there is a high density of valence electrons throughout the solid. Simple model: $+ve$ ion cores immersed in a uniform electron gas.

It would be nice to illustrate these distributions graphically (see for example Ashcroft and Mermin, p. 378).

(e) The FORTRAN language enables many simple formulae to be translated straightforwardly because the various arithmetic operations have the same priority as in mathematics. For example, multiplication and division are performed before addition and subtraction, so that $\frac{a}{b}+c$ is translated as `a/b + c`. The choice of `*` to denote multiplication and `/` to denote division also aids readability.

Brackets may be used exactly as in mathematics to change the interpretation of an expression; $\frac{a}{b+c}$ is translated as `a/(b + c)`.

FORTRAN's operators also have the normal associativity: $a-b-c$ translates into the FORTRAN `a - b - c`, and e^{x^2} to `e ** x ** 2`, with the correct meanings of $(a - b) - c$ and $e^{(x^2)}$.

Many of the built–in functions also have sensible names (although additional brackets are required around the argument); $\sin x$ is written `sin (x)`, $\sqrt{x}$ as `sqrt (x)`.

(f) 0.1 nm to 1.0 nm: Scale of interatomic separation. *Ab–initio* methods used for calculating the interatomic potential, relevant for estimation of cohesive energy or elastic properties for example.

1.0 nm to 10 nm: Scale of nucleation events, possibly modelled by molecular dynamic simulation of atomic or molecular motion.

10 nm to 1 mm: precipitates in alloys. Microstructural modelling of nucleation and growth rates will predict the evolution of yield stress on annealing.

10 mm to 1 mm: Grain diameters in alloys. Modelling of grain growth can predict the evolution of grain structure on annealing. Modelling can be by a variety of methods (vertex model, Monte-Carlo, front tracking)

1 mm to 1 cm: Possible scale of cracks. Linear-elastic fracture mechanics would be used to calculate the likelihood of brittle fracture.

1 cm to 1 m: Calculation of stress distributions in components, for example relevant for calculating the likelihood of fracture. Use of finite-element methods.

(g) The simplest case is when all the grain boundaries have the same energy; then they must meet at 120° junctions from the balance of forces. With 120° junctions, grains with fewer than 6 sides will have convex sides the curvature of which acts to force their migration inwards. The converse is true for grains with more than 6 sides. The shrinking grains ultimately disappear, reducing the total population of grains and thereby increasing the average grain size. The grain–diameter distribution is typically log–normal, and remains so during grain growth (*i.e.* there is self–similarity of the grain structures).

(h) The choice of time step length is crucial to achieving an efficient MD simulation. Ideally, it is desirable to make it as long as possible, so that the greatest amount of real time can be simulated for a given amount of computational effort. Too short a time step, and the phase space of the system will be sampled inefficiently. However, if the time step is made too long then the conserved quantities in the simulation (*e.g.* energy or temperature) may start to fluctuate wildly, eventually leading to catastrophic instability (‘blowing up’). This is because the trajectories of the particles are extrapolated into regions where the potential energy is very high, for example if the particles overlap. A general rule of thumb is that the time step should be comparable in magnitude to either the mean time between collisions in an atomic fluid, or one tenth of the fastest period of motion in a flexible macromolecule. However, the precise value of time step which can be used is very sensitive to the individual conditions under which the simulation is carried out, and must be tuned appropriately to maximise efficiency.

A satisfactory answer will include most of the preceding points, but extra marks should be allocated for a discussion of discrete nature of the integration algorithm. The fact the equations of motion are being integrated numerically will lead to truncation errors which will cause the particle trajectories to diverge exponentially fast from the continuous solutions. Increasing the order of the integration scheme and reducing the length of the time step will help to slow this effect, but in the end even the most accurate schemes will introduce significant errors in the trajectories. Fortunately, it turns out that provided the integration scheme is symplectic (*i.e.* roughly speaking, it obeys time reversal symmetry) then the values of the conserved quantities (*e.g.* energy, temperature, *etc.*) fluctuate about the true mean value, with no appreciable drift. The magnitude of these fluctuations will be proportional to the order of the scheme (Δt^4 for the Verlet leapfrog method) which is normally sufficient to ensure that they are less significant than the effects of over-extrapolating particle motion discussed above.

(i) The function to be maximised is q, so it is necessary to eliminate the free variable t, using the constraint that the material must not fail. Setting the wall stress equal to the yield strength gives

$$\sigma_Y = P\frac{r}{t} \qquad \text{so that} \qquad t = \frac{Pr}{\sigma_Y}$$

Substituting for t then gives

$$q = \lambda\frac{\Delta T}{t} = \frac{\Delta T}{Pr}(\lambda\sigma_Y).$$

It follows that $M = \lambda\sigma_Y$ must be maximised to achieve the greatest heat flux.

(j) Imagine the growth of a precipitate which is isolated from the matrix by an interface. There are three distinct quantities to consider: the precipitate, matrix and interface. The interface can be described as an evolving surface whose motion is controlled according to the boundary conditions consistent with the mechanism of transformation. The interface in this mathematical description is simply a two–dimensional surface with no width or structure; it is said to be a *sharp interface.*

In the phase–field method, the state of the entire microstructure is represented continuously by a single variable known as the *order parameter* ϕ. For example, $\phi = 1$, $\phi = 0$ and $0 < \phi < 1$ represent the precipitate, matrix and interface respectively. The latter is therefore located by the region over which ϕ changes from its precipitate–value to its matrix–value (Fig. 2). The range over which it changes is the *width* of the interface. The set of values of the order parameter over the whole microstructure is the *phase field.*

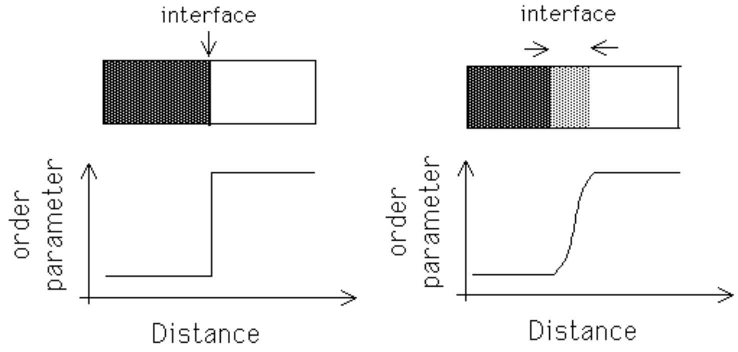

Fig. 2: (a) Sharp interface. (b) Diffuse interface.

SECTION B

2. Pair potential V is a potential between two atoms that depends only on their distance r apart.

Mathematically $V(r)$ can be represented as the second term in the many–body expansion of the general potential.

Main property: $V(r)$ has spherical symmetry which implies a central force law.

Because of spherical symmetry, the materials to which it can be applied reliably are molecular solids and ionic solids. In both cases the valence electron distributions are spherical or near-spherical.

To apply a pair potential to a metal would ignore the volume dependence of the delocalised electron gas (better to use embedded atom or bond order potentials which take this into account and are effective many body potentials).

Ignoring the energy of the electron gas has a significant effect on the elastic properties of metals. In particular, it incorrectly predicts that $c_{12} = c_{44}$ which is not observed.

Calculation, Part (i)

bcc structure has 8 nearest neighbours at $r_1 = a\sqrt{3}/2 = 2.482$Å, 6 second nearest neighbours at $r_2 = 2.866$Å, and 12 third nearest neighbours at $r_3 = a\sqrt{2} = 4.053$Å. (2 marks)

Since $V(r) = 0$ for $r > 3.44$Å, only 1st and 2nd near neighbour bonds contribute to the total energy of the metal.

The energy to remove an atom from the metal equals $8V(r_1) + 6V(r_2)$.

$$\begin{aligned} 8V(r_1) + 6V(r_2) =& 8[-0.639(2.482 - 3.116)^3 + 0.478(2.482) - 1.582] \\ &+ 6[-0.639(2.866 - 3.116)^3 + 0.478(2.866) - 1.582] \\ =& -3.074 \text{ eV} \end{aligned}$$

Assuming the atom reforms half its bonds on the surface (*e.g.* at a ledge) then the vacancy formation energy = 3.074/2 = 1.537 eV

Calculation, Part (ii)

1st nearest neighbour divacancy is along $< 1\ 1\ 1 >$. The energy to remove this divacancy from the metal equals

$$8V(r_1) + 6V(r_2) + 7V(r_1) + 6V(r_2) = -5.915 \text{ eV}$$

Assuming both atoms separately reform half their bonds on the surface, then the divacancy formation energy equals 5.915 – 3.074 = 2.841 eV

2nd nearest neighbour divacancy is along $< 1\ 0\ 0 >$ The energy to remove this divacancy from the metal equals:

$$8V(r_1) + 6V(r_2) + 8V(r_1) + 5V(r_2) = -5.946 \text{ eV}$$

Assuming both atoms separately reform half their bonds on the surface, then the divacancy formation energy equals 5.946 – 3.074 = 2.872 eV

3rd nearest neighbour divacancy is along $< 1\ 1\ 0 >$ The energy to remove this divacancy from the metal equals:

$$8V(r_1) + 6V(r_2) + 8V(r_1) + 6V(r_2) = -6.148 \text{ eV}$$

Assuming both atoms separately reform half their bonds on the surface, then the divacancy formation energy equals 6.148 – 3.074 = 3.074 eV

Hence the 1st nnb $< 1\ 1\ 1 >$ divacancy should be most stable (marginally) according to this pair potential. However, factors ignored include

atomic relaxation effects
temperature (entropic) effects
empirical nature of the pair potential

3. A thermodynamic function of state is independent of the path by which that state is reached. Quantities such as internal energy U, enthalpy H, pressure P, volume V are functions of state so that an integral of any of these quantities around a closed loop leads to no change. On the other hand, the heat q absorbed by a system during a change of state is very clearly a function of the path rather than the initial and final states alone. This is evident from the example below.

In the example of oxidation of hydrogen whose ΔH°_{298} is given and we wish to calculate ΔH°_T for the reaction:

$$\mathrm{H_2(g)} + \frac{1}{2}\mathrm{O_2(g)} = \mathrm{H_2O(g)},$$

We can take the reactants and form the product at 298 K and then heat the product to any temperature T or else we can heat the reactants to the temperature T from 298 K and then let the reaction take place at the temperature T. Both paths should result in identical enthalpies. The above scheme can be represented schematically as shown:

$$\begin{tikzcd}
H_2(g) + \frac{1}{2}O\ (g) \arrow[r, "\Delta H^\circ_{298}"] \arrow[d] & H_2O\ (g) \arrow[d] \\
H_2(g) + \frac{1}{2}O\ (g) \arrow[r, "\Delta H^\circ_{T}"] & H_2O\ (g)
\end{tikzcd}$$

$$\Delta H^\circ_{298} + \int_{298}^{T} c_P(H_2O) \ \ dT = \int_{298}^{T} c_P(H_2) \ \ dT + \frac{1}{2}\int_{298}^{T} c_P(O_2)\ dT + \Delta H^\circ_T$$

Therefore,

$$\Delta H^\circ_T = \Delta H^\circ_{298} + \int_{298}^{T} \Delta c_P \ \ dT$$

where

$$\Delta c_P = c_P(H_2O) - c_P(H_2) - \frac{1}{2}c_P(O_2)$$

4. Dissipative particle dynamics, introduced by Hoogerbrugge and Koelman in 1992, is a relatively recent off–lattice mesoscale method for simulating block copolymers, amphiphiles and other systems in which the time and length scales of the phenomena of interest are substantially longer and larger than could be accessed using atomistic simulation. In addition, DPD correctly takes into account hydrodynamic forces between particles which are thought to play an important role in the nucleation and growth of mesophase structures.

   Conceptually, DPD is a coarse-grained version of MD in which groups of atoms are treated as single particles whose internal degrees of freedom are assumed to be in equilibrium over each DPD time step. The net result of interactions between adjacent particles is averaged into dissipative and random (Brownian) forces which act pairwise between their centres of mass. These two forces obey a fluctuation–dissipation theorem so that an equilibrium temperature is established in the simulation. The chemical interactions between the different groups are then superimposed on top of this by introducing pairwise acting conservative forces between the clusters.

   The implications of the fluctuation-dissipation theorem on the mass transport in a DPD simulation is the relation between the diffusion coefficient and the magnitude of the fluctuations of particle displacements, *i.e.*

$$D = \left\langle (\Delta x)^2 \right\rangle / 2\Delta t$$

where Δt is some interval of time over which the movement is observed. The fact that all forces in a DPD simulation are pairwise acting is very important because it means that momentum is conserved by each collision, and therefore the macroscopic behaviour will be hydrodynamic (unlike MD or Brownian dynamics). In the presence of a sufficiently small perturbing field (which could be gravitational), the measurement of the diffusion coefficient via the fluctuation-dissipation theorem will be essentially unaffected. Linear response theory gives a straightforward way to calculate the magnitude of the change due to the field while the perturbation remains small (see following part of question). However, once the field strength becomes too high, or the particle motion is observed over long times, then the departure from equilibrium behaviour will become apparent, and a Green–Kubo type relation will be required to calculate the mass transport coefficients.

Fluctuation–dissipation theorem gives

$$\left\langle (\Delta x)^2 \right\rangle / 2\Delta t = \left\langle \{\Delta x_0 + (g/\xi)\Delta t\}^2 \right\rangle / 2\Delta t$$

Multiplying out and identifying $D_0 = \left\langle (\Delta x)^2 \right\rangle / 2\Delta t$, we obtain:

$$D = D_0 + (g/\xi)^2 \Delta t/2 + (g/\xi)\left\langle \Delta x_0 \right\rangle$$

and since $\left\langle \Delta x_0 \right\rangle = 0$

for a random walk, then this simplifies to:

$$D = D_0 + (g/\xi)^2 \Delta t/2$$

5. Generic attributes for selecting primary shaping processes may be classified into: (i) physical attributes (size, minimum section, roughness, tolerance); (ii) economic attributes (capital cost, economic batch size); and (iii) classes of materials that the process can be used with, and classes of shapes that the process is able to produce.

Material property databases can be generic across all materials since the majority of properties apply to every material (mechanical, thermal, electrical etc). Processes subdivide at a high level into classes of process which are physically quite distinct (shaping, joining, surface treatment), in which case there are few attributes which are generic to every type of process. One clear distinction for example is that shaping processes primarily apply to materials, while secondary processes such as joining and surface treatment apply to components.

C_L is the distributed cost, *i.e.* that which is charged at an hourly rate (labour, overheads, power, and an equivalent rental cost for the use of capital equipment) - it is divided by the production rate to give a contribution per part.

C_C is the dedicated cost, *i.e.* primarily for tooling written off on the process - it is divided by the batch size to give a contribution per part.

Process modelling can offer the following benefits in the context of selection of process in design:

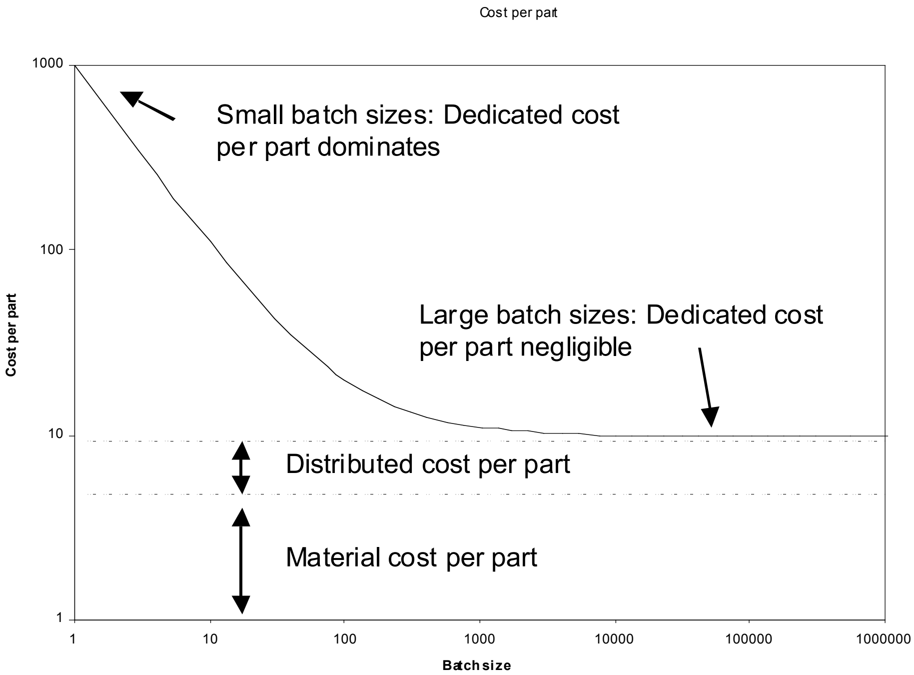

– capture the coupling between parameters of material, process and design (with a different sub-model for each competing process, but with the output from each model being common to all, to provide the discrimination needed for a given design requirement);

– enable co–selection of material and process (*e.g.* considering the effect of each process on all possible compositions, and making an optimal selection of material in view of the expected processability);

– provides feedback to the designer, in terms of suggested operating conditions for trials with each acceptable process, or prompting design changes which would enhance process speed or quality;

– provide a technical basis for selection decisions when empirical data are sparse, by interpolating between known combinations of conditions (or even between materials);

– connects sequential aspects of the selection procedure (*e.g.* estimates of processing speed for each viable process variant feed forward to cost estimates) .

SECTION C

6. In the context of molecular simulation, mechanical quantities are defined as those state functions whose expectation values can be computed by averaging over all the microstates of a system:

$$< Q >= \frac{1}{Z} \sum_i Q_i \exp\{-\beta E_i\}$$

Examples of mechanical quantities are the internal energy, enthalpy, pressure and volume, *i.e.* quantities that do not depend on the entropy of the system. Thermal quantities, such as entropy or free energy, cannot be computed as an average over microstates as they depend on the volume of phase space accessible to the system. In computer simulations, as in real life, the free energy of a system is minimised at equilibrium, and so it is not possible to measure it directly in a single run.

Instead, a reversible thermodynamic path must be constructed between some reference state of known free energy and the state under consideration. The change in free energy along that path can then be evaluated by thermodynamic integration. It is desirable to start with a reference state which is close in phase space to the actual state in order to minimise the number of simulations which need to be performed to carry out the integration, although there are very few suitable reference states for which the free energy is known a priori. One such state is the ideal gas, the other is the low temperature harmonic crystal. The former is suitable for considering condensation of a gas into a liquid with a known equation of state, and the latter might be used for computing the free energy of a particular solid state.

Since coexistence curves occur when the free energies of two or more phases become equal, it is possible to locate the coexistence point by using thermodynamic integration to calculate the conditions under which this equality is satisfied. This approach is preferred to direct simulation of the phases in coexistence, as the simulations will be dominated by the presence of interfaces even for (computationally speaking) large numbers of particles. A superior candidate will point out that there are specialist Monte Carlo techniques for dealing with liquid-vapour and liquid-liquid equilibria (Gibbs ensemble) but for solid-liquid equilibria thermodynamic integration is much more efficient as particle creation and annihilation within a dense phase is problematic.

(i) To find the Helmholtz free energy for a system with fixed number of particles at fixed temperature, we note that:

$$P = -\left(\frac{\partial F}{\partial V}\right)_{NT} \qquad \text{so that} \qquad \Delta F = -\int_{V_1}^{V_2} P \, dV$$

Hence we need to measure the pressure at each point between V_1 and V_2. A suitable computational methodology would be a series of NVT (or Metropolis) Monte Carlo simulations. The system is prepared in a random configuration with fixed volume using periodic boundary conditions, and its internal energy is evaluated. A random, ergodic perturbation is applied (*e.g.* particle translation) and the energy of the new state is compared to the old one. If the new energy is lower, the move is accepted automatically. If it is higher, the move is accepted with probability $\exp[\beta(E_{new} - E_{old})]$. The process is iterated to equilibrium, and the pressure on the cell walls is calculated. An alternative methodology would be to use NVT Molecular Dynamics. However, since MD samples naturally from the NVE ensemble, the use of a suitable thermostat would be required which adds to the computational burden of the simulation. As we are only seeking the equilibrium pressure of the system at a particular volume, the dynamical behaviour of the system is irrelevant, and a MC simulation is more efficient.

(ii) Plot $\ln(V_m)$ versus $\ln(P)$ and calculate best fit line with gradient β and intercept $\ln(\alpha)$, gives $\beta = 1.195$ to three significant figures.

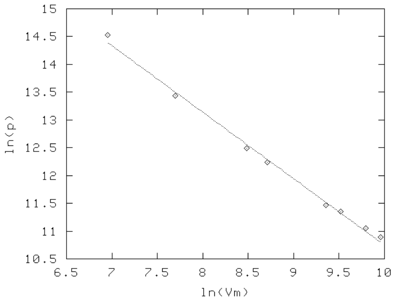

(iii)

$$\Delta F = -\int_{V_1}^{V_2} P\, dV = -\int_{V_1}^{V_2} \alpha V_m^{\beta}\, dV_m = \left[\alpha \frac{V_m^{\beta+1}}{\beta+1}\right]_{V_2}^{V_1}$$

$$= \frac{7.29 \times 10^8}{0.195}\left[(0.105 \times 10^4)^{-0.195} - (2.104 \times 10^4)^{-0.195}\right] \times 10^{-3}$$

$$= 428\,\mathrm{kJ\,mol^{-1}}$$

(iv) If the gas had condensed, there would have been a discontinuity in the P–V curve, and the viral expression used in part (ii) would have been inappropriate. The thermodynamic integration required to calculate the free energy change would have to be done numerically.

7. The fact that in addition to the new solid phase, an interface has to be created requires an additional undercooling to compensate for its defect energy. This is expressed in nucleation theory.

   Nucleation occurs by random hetrophase fluctuation in which a small volume of say β is created from the parent phase α. The new particle is surrounded by an α/β interface. For a spherical particle of radius r, the resulting change in free energy is

$$\Delta G = -\frac{4}{3}\pi r^3(\Delta G_V - \psi) + 4\pi r^2\gamma$$

   which on differentiation yields a maximum which is G^*:

$$G^* \propto \frac{\gamma^3}{(\Delta G_V - \psi)^2}$$

   where ΔG_V is the magnitude of the change in free energy per unit volume of β, ψ is the elastic strain energy and as usual, γ is the interfacial energy per unit area. G^* is the activation energy for nucleation. Note that $\psi = 0$ since we consider nucleation in a fluid.

   During transformation in extended space, particles can nucleate and grow in all regions irrespective of whether that space represents the parent or product phase.

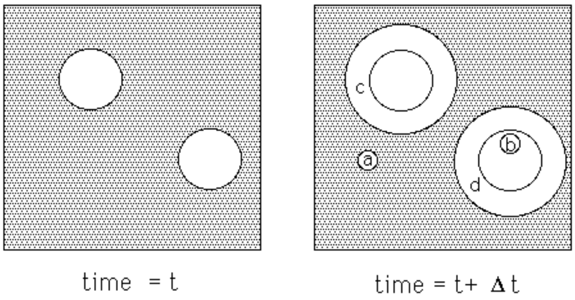

Fig. 3: An illustration of the concept of extended volume. Two precipitate particles have nucleated together and grown to a finite size in the time t. New regions c and d are formed as the original particles grow, but a & b are new particles, of which b has formed in a region which is already transformed.

Referring to Fig. 3, suppose that two particles exist at time t; a small interval δt later, new regions marked a, b, c & d are formed assuming that they are able to grow unrestricted in extended space whether or not the region into which they grow is already transformed. However, only those components of a, b, c & d which lie in previously untransformed matrix can contribute to a change in the real volume of the product phase (α) :

$$dV^\alpha = \left(1 - \frac{V^\alpha}{V}\right) dV_e^\alpha$$

where it is assumed that the microstructure develops at random. The subscript e refers to extended volume, V^α is the volume of α and V is the total volume. Multiplying the change in extended volume by the probability of finding untransformed regions has the effect of excluding regions such as b, which clearly cannot contribute to the real change in volume of the product. For a random distribution of precipitated particles, this equation can easily be integrated to obtain the real volume fraction,

$$\frac{V^\alpha}{V} = 1 - \exp\left\{-\frac{V_e^\alpha}{V}\right\}$$

Since there is no nucleation, the extended volume of the transformed phase is simply

$$V_e^\alpha = N\pi\frac{4}{3}G^3t^3$$

assuming spherical particles. Using the earlier relationship between extended and real space, it follows that

$$\xi = 1 - \exp\{-kG^3t3\}$$